Bolt loosening analysis and diagnosis by non-contact laser excitation vibration tests

Feblil Huda[#1], Itsuro Kajiwara[#2], Naoki Hosoya[#3], Shozo Kawamura[#4]

#1
Graduate Student
Division of Human Mechanical Systems and Design, Hokkaido University
N13, W8, Kita-ku, Sapporo 060-8628, Japan
Phone: +81-11-706-6392, Fax. +81-11-706-6390
E-mail: feblilhuda@ec.hokudai.ac.jp

Junior Lecturer
Department of Mechanical Engineering, University of Riau
Kampus Bina Widya, Jl. HR Subrantas km 12,5 Pekanbaru 28293, Riau, Indonesia

#2 (Corresponding author)
Professor
Division of Human Mechanical Systems and Design, Hokkaido University
N13, W8, Kita-ku, Sapporo 060-8628, Japan
Phone: +81-11-706-6390, Fax. +81-11-706-6390
E-mail: ikajiwara@eng.hokudai.ac.jp

#3
Associate Professor
Department of Engineering Science and Mechanics, Shibaura Institute of Technology
3-7-5 Toyosu, Koto-ku, Tokyo 135-8548, Japan
Phone: +81-3-5859-8055, Fax. +81-3-5859-8001
E-mail: hosoya@sic.shibaura-it.ac.jp

#4
Professor
Department of Mechanical Engineering, Toyohashi University of Technology, Hibarigaoka 1-1, Tempaku, Toyohashi, Aichi 441-8580, Japan
Phone +81-532-44-6674, Fax.+81-532-44-6674
E-mail: kawamura@me.tut.ac.jp

Abstract:

In this paper, a vibration testing and health monitoring system based on an impulse response excited by laser ablation is proposed to detect bolted joint loosening. A high power Nd: YAG pulse laser is used to generate an ideal impulse on a structural surface which offers the potential to measure high frequency vibration responses on the structure. A health monitoring apparatus is developed with this vibration testing system and a damage detecting algorithm. The joint loosening can be estimated by detecting fluctuations of the high frequency response with the health monitoring system. Additionally, a finite element model of bolted joints is proposed by using three-dimensional elements with a pretension force applied and with contact between components taken into account to support the bolt loosening detection method. Frequency responses obtained from the finite element analysis and the experiments using the laser excitation, are in good agreement. The bolt loosening can be detected and identified by introducing a damage index by statistical evaluations of the frequency response data using the Recognition-Taguchi method. The effectiveness of the present approach is verified by simulations and experimental results, which are able to detect and identify loose bolt positions in a six-bolt joint cantilever.

Keywords: bolt loosening, laser excitation, finite element model, high frequency response, fault diagnosis, RT method.

1. Introduction

Bolted joints are widely employed when joining two or more parts together in mechanical products and structures due to the ease of disassembly for maintenance. However, bolted joint failures, including self-loosening, shaking apart, slippage, stress cracking due to fatigue, and breaking due to corrosion [1], are frequent, and it has been suggested that most failures of bolted joint are caused by loosening [2]. For this reason, bolt loosening has become an important research area in mechanical engineering in efforts to prevent failures in a variety of mechanical applications.

Several methods of bolt modeling have been studied by previous researchers. Kim proposed four kinds of finite element models to model structures with bolted joints [3]. Ahmadian developed a non-linear generic element formulation for modeling bolted lap joints [4]. Bograd gave an overview of different approaches to modeling the dynamics of mechanical joints in assembled structures where the finite element method is based on three different approaches: node-to-node contact using the Jenkins frictional model, thin layer elements, and zero thickness elements [5]. That research has been concerned with the bolted joint modeling in commonly occurring conditions only. However, modeling of bolted joints that undergo loosening is necessary to underpin bolt loosening detection methods.

Detecting the loosening of bolted joints is important to ensure the proper functioning of structures or subassemblies. The process to implement a method of damage detection is generally referred to as structural health monitoring [6]. Several approaches have been investigated in regard to the detection of loosening in bolted joints, especially those using impedance [7,8], electrical conductivity [9], and vibration measurements [10]. Vibration based approaches have commonly involved contact excitation, using piezoelectric materials or impulse hammers to excite a structure to determine the frequency response. However, using piezoelectric components require these to be firmly attached to structures and larger sized piezoelectric components may need to be bolted to a structure. Hammering methods require specially trained technicians and are time consuming. Further, the reproducibility of input characteristics with hammering is poor, while measurements of dynamics characteristics require high reproducibility to be optimally useful. These issues have led to research into non-contact excitation methods with better reproducibility. Vibration measurement systems using non-contact laser excitation can guarantee a very high degree of measurement reproducibility [11-13].

Lasers are used in a variety of applied technologies due to their high coherence and energy density. There are two reasons for employing lasers as the source of the excitation in this study. Besides providing a high degree of measurement reproducibility, laser excitation also allows measurement of vibrations at high frequencies. Specifically, it has been reported that changes in natural frequencies and mode shapes are more prominent in modes at higher frequencies when damage occurs within a structure [14]. This would make it a suitable excitation method for bolt loosening detection.

In this study, a finite element modeling method for bolted structures is proposed and a laser health monitoring technique for detecting bolt loosening in joint structures is developed. Vibration testing based on non-contact impulse excitation using laser ablation is conducted. A high-power Nd: YAG pulse laser is used for producing an ideal impulse on the structural surface. The high frequency response of the structure is then measured. Loose bolt conditions are simulated by reducing the torque used to tighten a bolted joint assembly. The change in vibration characteristics due to the bolt loosening affected in this manner in the high frequency region can be extracted by the laser excitation vibration measurement. The research approach is supported by a finite element model of bolted joints that undergo loosening, which is verified by vibration testing based on non-contact impulse excitation using laser ablation. Finally, a method for loose bolt detection is proposed by applying a statistical evaluation of the Recognition-Taguchi (RT) method to a six-bolt joint cantilever with a loose bolt.

2. Vibration testing system using laser ablation

2.1 Laser ablation

The principles of non-contact excitation forces generated by laser ablation are used in this research. The process of the laser ablation is presented in Fig.1. When a laser beam is irradiated on a metal surface, it will be absorbed by the metal, and the atoms absorbing the laser light release ions. The absorption of the energy in the laser beam by metal will also generate high-temperature plasma, and large quantities of particles are then released (in the form of a plume) from the metal (Fig. 1(a)). Momentum is then generated when a mass Δm released at a velocity v from the metal, represented by Δmv, and this expresses the laser induced impulse.

To generate a larger excitation force on the structure, a water droplet is placed on the metal surface during laser ablation as shown in Fig. 1(b). The laser ablation occurs on the metal surface when the laser passes through the water droplet and reaches the metal surface. In addition to the release of particles from the metal surface, the water droplet evaporates with the rapid increase in the temperature of the metal surface, releasing the mass ΔM of the water droplet at a velocity V. The total resulting momentum is $\Delta mv+\Delta MV$, resulting in a larger impulse with than without the water droplet (Fig. 1(b)). The particles and water vapor are released radially from the metal surface, and the direction of the impulse only comprises the element that is normal to the metal surface. This impulse constitutes the excitation force on the structure.

2.2 Pulse laser

High-frequency vibration measurement of structures with natural frequencies in the high frequency range may be conducted by laser excitation vibration testing. A vibration testing arrangement using a high-power pulse laser is shown in Fig. 2. An Nd: YAG laser (Continuum Surelite III) with a

wavelength of 1064 nm, maximum output of 1 J, and a pulse width of 5 ns is installed on an optical table. The beam is focused at a spot on the structure, and has a diameter of 25 μm using a convex lens with the focal length 100 mm to cause the laser ablation.

2.3 Measurement and analysis of output

To measure the output response, accelerometers are attached to the measuring points of the structure with an adhesive. A spectrum analyzer (A/D; NI-4472B, Software; Catec CAT-System) is used for measuring the acceleration response and analysing the Fourier spectrum of the structure. The maximum measurement frequency is set to 40 kHz in this study. Based on the specifications, the natural frequency of the accelerometers used in this experiment is above 50 kHz, and experiments verified that the natural frequency of the accelerometers is sufficiently higher than the maximum measurement frequency of 40 kHz.

The laser excitation realizes an ideal impulse excitation, making it possible to use the Fourier transform of the output response for the evaluation of the vibration characteristics of the system as the frequency response function. The Fourier transforms of time histories of an input force $f(t)$ and output response $x(t)$ into the frequency domain are described by

$$F(\omega) = \int_{-\infty}^{\infty} f(t) e^{-j\omega t} \mathrm{d}t \tag{1}$$

$$X(\omega) = \int_{-\infty}^{\infty} x(t) e^{-j\omega t} \mathrm{d}t \tag{2}$$

The output response $x(t)$ can be expressed by the convolution integral with an impulse response function $h(t)$ of the system:

$$x(t) = \int_{-\infty}^{\infty} h(t-\tau) f(\tau) \mathrm{d}\tau \tag{3}$$

The Fourier transform of Eq.(3) results in

$$X(\omega) = H(\omega) F(\omega) \tag{4}$$

where, $H(\omega)$ is the frequency response function of the system. When $f(t)$ is an impulse force, ideally the Dirac delta function, the Fourier transform $f(t)$ becomes $F(\omega) = 1$, and Eq.(4) is expressed by

$$X(\omega) = H(\omega) \tag{5}$$

The result is that the Fourier transform of the response $x(t)$ becomes the frequency response function.

3. Finite element analysis of bolted joint

With the aim of developing the finite element model of bolted joints, a simple three-dimensional finite element model of a bolted joint with solid element formed by one bolt-nut and two flanges was used in the bolted joint modeling. This model allowed an independent study of the normal and loose conditions to be considered for the model. The normal condition represents the bolt with standard

tightening torque, and loose condition occurred when the bolt get lower tightening torque than standard. A more complex bolted joint was next modeled for the application of the proposed method to more complex structures.

3.1 Model description

The finite element analysis software ANSYS 14.0 has been used to model bolted joint with pretension force and mating part contact. The one-bolt joint model is constructed in form of cantilever, where one of the flanges is fixed, as shown in Fig.3. The SOLID186 element of ANSYS which is defined by twenty nodes, having three degrees of freedom at each node is used to construct physical model of bolted joint. The total number of nodes and elements are 29635 and 5412, respectively.

In the model, the tightening torque applied to the bolt is converted to a pretension force. The relationship between the given tightening torque and the arising pretension force is described by

$$F = \frac{T}{K \times d} \tag{6}$$

where *F, T, K* and *d* are the pretension force, the tightening toque, torque coefficient and the nominal diameter of bolt, respectively.

The pretension force is applied by using pretension element PRETS179 in ANSYS, where the value of the pretension force can be applied directly to the bolt. The pretensions of the bolt will be varied from standard pretension which represents normal condition to lower ones which represent loosening conditions. The contact modeling is presented by surface-surface contact elements, which is a pair, the contact element CONTA174 and the target element TARGE170. The contact elements are applied to the interfaces between bolt head and upper flange, nut and lower flange, and between upper flange and lower flange. There are three types contact used in this model:

a) Bonded, where no sliding or separation between interfaces or edges is allowed.
b) Frictional, where two contacting interfaces may be subject to shear stresses up to a specified magnitude across the interface before sliding occurs.
c) No separation, where separation of the interfaces in contact is not allowed, but where small amounts of frictionless sliding may occur along the contacting interfaces.

The simple bolted joint connection used in this study is composed of two aluminum flanges, each 10 mm thick and joined with a stainless steel M10 bolt. The material of the bolt and the flanges are assumed to exhibit linear elastic behaviors during clamping. The mechanical properties of the material used in the linear elastic finite element analysis for the bolt are a Young's modulus of 193 GPa, a Poisson ratio of 0.31, and a mass density of 7750 kg/m^3, for the flanges the Young's modulus is 68 GPa, the Poisson ratio 0.33, and the mass density 2700 kg/m^3.

3.2 Determining contact condition between flanges

The static structural analysis with a given pretension force applied to the bolt was conducted to determine the contact type between the flanges which are subject to the pretension force. This analysis is also used to establish the initial conditions for the following analysis, the pre-stressed modal analysis.

To determine the contact type between the flanges, the region where the stresses due to the pretension that produced the clamping force are predominant is set so they may be considered to be bonded to each other. That region forms a conical shape and covers a range of $25^{o} \leq \alpha \leq 33^{o}$, as suggested by Osgood [15]. The bolt head and the nut are also assumed to be glued to the flanges due to the clamping force. A pretension force for the normal and loosened condition will be applied to the bolt. Table 1 shows the relationship between the given tightening torques and pretension forces arising in model.

Table 1 Relationship between tightening torques and pretension forces

Tightening Torque (Nm)	Pretension Force (N)	State
24.5	12260	Normal
20.0	10000	Loose
18.0	9000	Loose
15.0	7500	Loose
10.0	5000	Loose

The static structural analysis is then conducted with ideal conditions, where the entire contact area between the components of the bolted joint is assumed to be bonded. The stress and elastic strain data on the contact between the flanges are then obtained. By applying the conical shape suggested by Osgood, the values of the stress on the outer radius of the conical shape due to the normal pretension force are considered the basic values (benchmark) and the limits for the bonded area. The contact region with the value of stresses greater than or equal to the values of the benchmark becomes the bonded contact area, and the other contact areas will be frictional and no separation. This process is suggested in Fig.4, which also shows that in the case of a loose condition, the contact arrangement will change with the benchmark values of the stress.

Fig.5 shows stress distribution between flanges in contact used for determining the state of the bonded contact, and how to determine the limit of the contact area for bounded areas graphically when the benchmark values for stress is already established using the Osgood cone. By drawing a horizontal straight line based on the benchmark value which then crosses the curves of stress for every pretension force, the limits for bonded contact is determined by as the point directly below the point where the horizontal line touches the stress curve. In this way the bonded area between flanges with a pretension force of 12260 N is 5.5 cm to 15 cm, and it is 5.5 cm to 13.5 cm, 5.5 cm to 13 cm, 5.5 cm

to 12 cm, and 5.5 cm to 9.5 cm for pretension forces of 10000 N, 9000 N, 7500 N, and 5000 N, respectively. Using the elastic strain curve with the same procedure, will yield similar results as those for stress.

3.3 Frequency response analysis

To utilize the bolted joint model proposed in this study for a dynamic analysis, a series of frequency response analysis tests using the finite element method were carried out. The frequency response analysis was executed by applying pre-stressed modal analysis with initial conditions given by the results of the static structural analysis.

Some reports have found that nonlinear features like frictional contact elements cannot be counted in a modal analysis [3,16], and this has caused other research to employ linear contact for the modal analysis. In this study, the effects of the frictional contact are taken into account in dynamic analysis as pre-stressed modal analysis, in which the static structural analysis with contact element results in the stress and elastic strain which are maintained as initial condition of next analysis, modal analysis. Even though there is no direct effect of frictional contact in the modal analysis, using frictional contact will affect the static structural analysis as the initial condition of the pre-stressed modal analysis.

Several pre-stressed modal analysis are carried out for normal and loose conditions. The loose conditions are given by changing the value of the pretension force and the type of contact area.

3.4 Finite element model of generalize complex bolted joint

To further evaluate the modeling method of the finite element analysis that has been developed above for a simple one-bolt joint, a more complex bolted joint model was used to show the applicability of the method of the analysis. Here, a three-dimensional finite element model of a bolted joint which consists of two flanges and six bolts is built. The six-bolt joint is modeled as a cantilever with the same materials as the simple one. The dimensions in mm and the bolt numbering of the six-bolt joint model are shown in Fig.6.

Using the method applied to the simple one-bolt joint, a static analysis to determine contact area and a frequency response analysis were conducted. The normal condition was set by applying a tightening torque of 24.5 Nm to accord with a pretension force of 12260 N, and the loosening condition is adjusted by applying tightening torques of 20 Nm or 16.5 Nm for pretension forces of 10000 N or 8250 N, respectively. The list of damage cases considered here for the six-bolt model is provided in Table 2, where the applied tightening torque on each bolt is detailed for damage case.

Table 2 List of torques applied in damage cases for the six-bolt joint model

Condition	Tightening Torque (Nm)					
	Bolt 1	Bolt 2	Bolt 3	Bolt 4	Bolt 5	Bolt 6
Normal	24.5	24.5	24.5	24.5	24.5	24.5
Damage 1	20.0	24.5	24.5	24.5	24.5	24.5
Damage 2	24.5	24.5	24.5	20.0	24.5	24.5
Damage 3	24.5	24.5	24.5	24.5	20.0	24.5
Damage 4	16.5	24.5	24.5	24.5	24.5	24.5
Damage 5	24.5	24.5	24.5	16.5	24.5	24.5
Damage 6	24.5	24.5	24.5	24.5	16.5	24.5

4. Verification of the finite element model by laser excitation vibration measurements

In the laser excitation vibration tests, points for excitation and measurements were selected first, to ensure these points excite and measure most natural modes of excited structure. To verify the finite element model analysis by experiment, the excitation and measurement points for the one-bolt joint and a six-bolt joint are chosen, resulting in excitation points and measurement points as shown in Fig. 7. For the simple one-bolt joint, the tests are to be conducted in the vertical and horizontal directions, as suggested in Fig. 7(a) and Fig. 7(b), respectively. Since on a complex structure, it is unusual to conduct the vibration test in the horizontal direction of a joint, the test for the six-bolt joint will be carried out in the vertical direction only, as suggested in Fig. 7(c). The measurement point of the six-bolt joint model is directly behind the excitation point.

4.1 Frequency response on the one-bolt joint model

A vibration test by using the laser excitation without a water droplet was conducted for the one-bolt joint model. The tightening torques is applied by a digital torque wrench for normal condition and loose conditions. The variation conditions to the one-bolt joint model are explained in Table 1. In order to compare simulations and experimental results, the frequency response graphs of the two sets of results will be plotted together, to show the degree of agreement between the results and enable an evaluation of the adequacy of the proposed method in modeling bolted joint with one-bolt.

The frequency responses of the one-bolt joint in the normal condition are shown in Fig. 8. The frequency responses in the normal condition by simulation and experiment show good agreement, they have similar peaks and tendency over the whole frequency range. This good agreement can be seen both in the vertical and horizontal directions of tests.

Fig.9 shows the frequency response of the one-bolt joint with loose conditions in the vertical direction, and Fig.10 shows that in the horizontal direction. When the tightening torque is reduced, the resonance peaks in the frequency response shift to lower frequencies. This shift is significant at high frequencies, but it is not clear in lower frequencies. This is seen clearly when all frequency responses

with different tightening torque from normal condition to loosening conditions are plotted together. The frequency responses with different tightening torques obtained from the experiments in vertical and horizontal direction are shown in Fig. 11.

Fig. 11 shows that the change of natural frequency is more significant at high frequencies than at low frequencies. This is clearly shown when a bolted joint undergoes loosening, the stiffness of the joint is reduced, and the stiffness reduction leads the significant shift of the high frequency resonance peaks to lower frequencies.

The resonance peak shifts at high frequencies can also be considered from the vibration mode shapes. The principal vibration mode shapes of the one-bolt joint model in normal condition are shown in Fig. 12. At low frequencies including the modes 1, 3, and 4, the deformation around the bolt is not large. At high frequencies including modes 10, 14, and 16, the mode shapes are complicated, the bolt and the nut undergo the significant elastic deformation. This mode deformation of the bolt which has different pretension forces in each case of the loosening contribute more to the resonance peak shifts. This explains why the resonance peaks show significant changes at high frequencies rather than at low frequencies.

4.2 Frequency response on the six-bolt joint model

To check the integrity of the modeling and to ensure the aplicability of the laser excitation vibration test to more complex bolted joint, the simulation and the experiment on six-bolt joint are conducted. Fig. 13 shows a plot of the frequency response of the six-bolt joint in the normal condition. Frequency response for loose condition is presented in Fig. 14, where damage 1 and damage 5 as representation of loose condition based on damage cases on Table 2 are applied. The frequency response shows more resonance peaks in six-bolt joint model compared to that of one-bolt joint model in the range up to 40 kHz. The frequency response graph shows a good agreement between simulation and experiment. The results on six-bolt joint demonstrate that the proposed finite element model in this paper can be applied well to more complex bolted joint. The frequency responses with different tightening torques (normal and several damage cases) obtained from experiments in vertical direction is presented in Fig. 15.

The graph in Fig. 15 shows that the frequency response changed significantly at high frequencies due to bolt loosening. This is similar to that of the one-bolt joint. By this tendency in bolt loosening case, employing the laser excitation vibration measurement system in this research is definitely an appropriate decision, because the high frequency response can be precisely measured by this excitation/measurement. Bolt loosening detection has become much easier by evaluating high frequency response, because the significant response shift in high frequency will be easy to detect.

5. Bolt loosening detection approach

5.1 Damage detection method

The RT method is a statistical evaluation method used for detecting the loose bolts in this study, and is a type of Mahalanobis-Taguchi (MT) method used in the field of quality engineering as a pattern recognition method [17]. In this method, data is measured a number of times under identical conditions, and a unit space for the condition is defined. Information that forms the unit space is called a member. For members comprising a unit space, quantities known as the standard S/N ratio η and the sensitivity β are defined based on a concept of quality engineering [17]. These are then used to define the distance in relation to the unit space using the RT method. For unknown data, distances in relation to unit spaces are calculated and compared to determine to which unit space the unknown data belongs. A value belonging to a member and used in the calculations is referred to as an item. When n is the number of members, and k is the number of items, items are expressed as X_1, X_2, …, X_k, and their averages are expressed as m_1, m_2, …, m_k. Specifically:

$$m_i = \frac{1}{n}\left(X_{i1} + X_{i2} + \cdots + X_{in}\right) \tag{7}$$

Table 3 shows the relation between the items and their averages. The standard S/N ratio η and sensitivity β to each member of the unit space are obtained using the following equations. Using a linear equation L_1

$$L_1 = m_1 X_{11} + m_2 X_{21} + \cdots + m_k X_{k1} \tag{8}$$

The sensitivity $\beta_1$is obtained as

$$\beta_1 = \frac{L_1}{r} \tag{9}$$

where

$$r = m_1^{\ 2} + m_2^{\ 2} + \cdots + m_k^{\ 2} \tag{10}$$

The total variation S_{T1} and the variation $S_{\beta 1}$ of the proportional term are describe as

$$S_{T1} = X_{11}^{\ 2} + X_{21}^{\ 2} + \cdots + X_{k1}^{\ 2} \tag{11}$$

$$S_{\beta 1} = \frac{L_1^{\ 2}}{r} \tag{12}$$

The error variation S_{e1} and the error variance V_{e1} are obtained by

$$S_{e1} = S_{T1} - S_{\beta 1} \tag{13}$$

$$V_{e1} = \frac{S_{e1}}{k-1} \tag{14}$$

The S/N ratio η_1 is calculated as

$$\eta_1 = \frac{1}{V_{e1}} \tag{15}$$

Similar calculations are performed to obtain β and η for the second member, the third member, and so on until the nth member, and are listed in Table 4. The β and η are used to obtain the distance within the unit space. The S/N ratio η is not used directly, but is used as in the following equations and listed in Table 5.

$$Y_{1i} = \beta_i \tag{16}$$

$$Y_{2i} = \frac{1}{\sqrt{\eta_i}} \tag{17}$$

Table 3 Variables of members in a unit space

Member	$X1$	$X2$	...	Xk
1	$X11$	$X21$	...	$Xk1$
2	$X12$	$X22$	...	$Xk2$
⋮	⋮	⋮	⋮	⋮
n	$X1n$	$X2n$	...	Xkn
Average	$m1$	$m2$	...	mk

Table 4 η and β of the members in a unit space

Member	H	B
1	$\eta 1$	$\beta 1$
2	$\eta 2$	$\beta 2$
⋮	⋮	⋮
n	ηn	βn

Table 5 Y of the members in a unit space

Member	$Y1$	$Y2$
1	$Y11$	$Y21$
2	$Y12$	$Y22$
⋮	⋮	⋮
n	$Y1n$	$Y2n$

The data of the members of a unit space is consolidated in Y_1 and Y_2. Here, Y_1 represents sensitivity and Y_2 represents standard deviation. The RT method is applied to obtain the distance D for the unit space from the data for the n members in the unit space. A comparison is made with D to determine whether the distance in relation to the data is sufficiently large. The RT method calculates the variance and covariance of Y_1 and Y_2, and a variance–covariance matrix. The variance of Y_1 is represented by V_{11}, the covariance of $Y_1 \cdot Y_2$ is represented by V_{12}, the variance of Y_2 is represented by V_{22}, and the relationship $V_{21} = V_{12}$ is valid. If $\overline{Y_1}$ is the average of Y_1 and $\overline{Y_2}$ is the average of Y_2, then,

$$V_{11} = \frac{1}{n-1}\sum_{i=1}^{n}(Y_{1i} - \bar{Y}_1)^2 \tag{18}$$

$$V_{12} = \frac{1}{n-1}\sum_{i=1}^{n}(Y_{1i} - \bar{Y}_1)(Y_{2i} - \bar{Y}_2) \tag{19}$$

$$V_{22} = \frac{1}{n-1}\sum_{i=1}^{n}(Y_{2i} - \bar{Y}_2)^2 \tag{20}$$

Therefore, the variance–covariance matrix $\boldsymbol{V}$ is

$$\boldsymbol{V} = \begin{pmatrix} V_{11} & V_{12} \\ V_{12} & V_{22} \end{pmatrix} \tag{21}$$

and the cofactor matrix $\boldsymbol{A}$ of the variance–covariance matrix $\boldsymbol{V}$ is

$$\boldsymbol{A} = \begin{pmatrix} V_{22} & -V_{12} \\ -V_{12} & V_{11} \end{pmatrix} \tag{22}$$

The distance for the first member of the unit space is described by

$$D_1^2 = \frac{1}{2}\left[V_{22}\left(Y_{11} - \bar{Y}_1\right)^2 - 2V_{12}\left(Y_{11} - \bar{Y}_1\right)\left(Y_{21} - \bar{Y}_2\right) + V_{11}(Y_{21} - \bar{Y}_2)^2\right] \tag{23}$$

The distances D_2^2, D_3^2, …, and D_n^2 are obtained for the remaining members of the unit space. The square root of the average of D_1^2, D_2^2, …, and D_n^2 is the distance $\bar{D}$ from the zero point of this unit space; i.e.,

$$\bar{D} = \left\{\frac{1}{n}\left(D_1^2 + D_2^2 + \cdots + D_n^2\right)\right\}^{\frac{1}{2}} \tag{24}$$

The above information is used to examine whether an unknown data value is included in specific unit spaces. Here, using m_1, m_2, …, and m_k as the average of a specific unit space being examined, a linear equation

$$L = m_1 X_1 + m_2 X_2 + \cdots + m_k X_k \tag{25}$$

is applied to the unknown data X_1, X_2, …, and X_k, and the sensitivity β_o and the standard S/N ratio η_o is obtained.

$$\beta_o = \frac{L}{r} \tag{26}$$

$$\eta_o = \frac{1}{V_e} \tag{27}$$

where

$$r = m_1^2 + m_2^2 + \cdots + m_k^2 \tag{28}$$

$$S_T = X_1^2 + X_2^2 + \cdots + X_k^2 \tag{29}$$

$$S_\beta = \frac{L^2}{r} \tag{30}$$

$$S_e = S_T - S_\beta \tag{31}$$

$$V_e = \frac{S_e}{k-1} \tag{32}$$

Next, Y_{1o} and Y_{2o} for unknown data are obtained from β_o and η_o.

$$Y_{1o} = \beta_o \tag{33}$$

$$Y_{2o} = \frac{1}{\sqrt{\eta_o}} \tag{34}$$

From these relations, the distance in relation to the unknown data value is obtained using

$$D^2 = \frac{1}{2}\left[V_{22}\left(Y_{1o} - \bar{Y}_1\right)^2 - 2V_{12}\left(Y_{1o} - \bar{Y}_1\right)\left(Y_{2o} - \bar{Y}_2\right) + V_{11}(Y_{2o} - \bar{Y}_2)^2\right] \tag{35}$$

The D and $\bar{D}$ are compared to determine whether the unknown data value is included in the corresponding unit space. Now, the damage index (DI) which determines the condition of bolt, normal or not, is defined by

$$\text{Damage Index(DI)} = \frac{D}{\bar{D}} \tag{36}$$

If DI > 1, the bolt is in damage condition (loosening), and if DI ≤ 1, the bolt is in normal condition.

5.2 The location of excitation and measurement points

The excitation conditions must be designed to excite all vibration modes of the joint in the direction of the measurement, making it necessary to select a suitable position for the excitation. The characteristic change in the measured frequency responses should be sensitive to loosening of every bolt, making it necessary to locate the measurement points close to each of the bolts. The excitation and measurement points for bolt loosening detection are shown in Fig. 16.

6. Diagnosis results

By taking damage scenarios based on the damage cases on Table 2, vibration measurement by using laser excitation is conducted. Excitations are given on a point, and vibration measurement is conducted on several points close to the bolt which represent measurement on each bolt.

6.1 Diagnosis process

To create the unit spaces for diagnosis, the power spectra of responses in normal condition under identical conditions were measured a multiple number of times. In other words, the response varied slightly even in the same conditions due to slight differences in the actual state. For this purposes, the measurement process involved loosening all bolts after one measurement, refastening the bolts under the same tightening condition as before, and measuring the response under the same test condition. The process was repeated, and ten sets of power spectrum data for normal condition were measured. The measured data were analysed as follows with regards to data sample regions and data sample points for diagnosis:

1. A frequency range in high frequency from 12.5 kHz to 40 kHz is set within the range of interest to perform the diagnosis.
2. The range is divided into multiple sub-regions, where the frequency band of sub-regions in the data analysis was 125 Hz.
3. An average value is obtained as an item within each of the sub-regions.
4. The items are obtained within all the sub-regions.

The unit space in a member was created with the items in the member in the range of interest, and it was performed on normal condition only. This unit space was used to perform a comparison with unknown data and used for a diagnosis. The correlation between the data belonging to the unit space of normal condition and unknown data (loosening condition) in the same range of interest was evaluated with the damage index.

6.2. Results

To investigate the applicability of the diagnosis in this study, the power spectra of the responses were measured at six points, where each point had its position close to a bolt. Every point of measurement represents the measurement on each bolt, so there were six bolts and six points of measurement.

The measurements were conducted first for the normal condition to get the unit space that was constructed from ten sets of power spectrum data. The measurements for several damage conditions were then conducted to get one set of power spectrum data for each case of damage. By comparing the damage data with the unit space, a damage index was developed. The damage index for each bolt for the simulation and experiments is shown in Table 6 and Table 7, respectively.

Table 6 Damage index based on simulation

Case \ Position	Bolt 1	Bolt 2	Bolt 3	Bolt 4	Bolt 5	Bolt 6
Damage 1	36.00	14.00	14.60	11.90	18.00	6.32
Damage 2	16.86	16.82	15.08	55.68	14.08	14.27
Damage 3	15.75	15.65	15.90	16.15	17.30	16.30
Damage 4	56.70	20.74	20.05	31.20	27.80	10.30
Damage 5	25.22	19.30	25.88	40.03	16.51	18.97
Damage 6	25.73	26.05	24.54	28.90	33.10	27.70

Table 7 Damage index based on experiments

Case \ Position	Bolt 1	Bolt 2	Bolt 3	Bolt 4	Bolt 5	Bolt 6
Damage 1	10.40	7.00	1.60	0.67	0.45	0.41
Damage 2	0.45	2.20	0.44	5.47	1.62	0.62
Damage 3	1.80	2.20	3.11	2.38	7.76	2.56
Damage 4	29.30	9.10	5.30	3.20	2.53	2.86
Damage 5	0.58	1.88	0.32	5.93	4.70	2.39
Damage 6	3.73	3.25	7.54	0.82	11.43	3.77

Table 6 and Table 7 show that most of damage index numbers are greater than 1, which means that the damage condition (loosening) of the joint can accurately be detected in every position of measurement, and the highest value of damage index in the same damage case represents the position of the loose bolt. These results correspond to the scenario of the cases of loosening that has been designed in this research.

7. Conclusions

In this research, bolt loosening detection by vibration testing using non-contact laser excitation and a finite element model of bolted joint undergoing loosening were proposed to investigate modeling and detecting of bolt loosening on bolted structures. In addition, through a comparison between simulations and experimental results, the effectiveness and usefulness of the bolt model and loosening detection approach were confirmed.

To model a structure with bolted joints in a loosening condition, it is necessary to change the pretension force, and contact conditions between parts from the initial conditions. The frequency response analysis by pre-stressed modal analysis has shown that the proposed modeling method gives good agreement with the experimental results. The use of the laser excitation vibration measurement arrangement in this research enabled a high degree of measurement reproducibility; offering the promise that the quality and reliability of the bolt loosening detection methodology can be improved. Both the simulation and experimental results for the bolt loosening detection showed that various loosening states and their positions can be effectively identified by using the RT method as a frequency response based approach, which requires excitation at a point and measurements at several points close to the bolts.

Acknowledgements

This study was supported by the Grant-in-Aid for Scientific Research (A) (22246027), Grant-in-Aid for Young Scientists (A) (22686025) and Grant-in-Aid for Challenging Exploratory Research (24656158) from the Japan Society for the Promotion of Science. We hereby express our deep gratitude for this support.

References

[1] D.M. Peairs, G. Park, D.J. Inman, Practical issues of activating self-repairing bolted joints, Smart Mater. Struct. 13 (2004) 1414 - 1423.

[2] T. Yokoyama, M. Olsson, S. Izumi, S. Sakai, Investigation into the self-loosening behavior of bolted joint subjected to rotational loading, Engineering Failure Analysis 23 (2012) 35 - 43.

[3] J. Kim, C. J. Yoon, S. B. Kang, Finite element analysis and modeling of structure with bolted joints, Applied Mathematical Modeling 31 (2007) 895 - 911.

[4] H. Ahmadian, H. Jalali, Generic element formulation for modeling bolted lap joints, Mechanical Systems and Signal Processing 21 (2007) 2318 - 2334.

[5] S. Bograd, P. Reuss, A. Schmidt, L. Gaul, M. Mayer, Modeling the dynamics of mechanical joints, Mechanical Systems and Signal Processing 25 (2011) 2801 - 2826.

[6] C.R. Farrar, K. Worden, An introduction to structural health monitoring, Philos. Trans. R. Soc. A 365 (2007), 303 - 315.

[7] D.M. Peairs, G. Park, D.J. Inman, Improving accessibility of the impedance-based structural health monitoring method, Intell. Mater. Syst. Struct. 15 (2004) 129 - 139.

[8] S. Ritdumrongkul, M. Abe, Y. Fujino, T. Miyashita, Quantitative health monitoring of bolted joints using a piezoceramic actuator sensor, Smart Mater. Struct. 13 (2004) 20 - 29.

[9] I. Argatov, I. Sevostianov, Health monitoring of bolted joints via electrical conductivity measurements, International Journal of Engineering Science 48 (2010) 874 - 887.

[10] M.D. Todd, J.M. Nichols, C.J. Nichols, L.N. Virgin, An assessment of modal property effectiveness in detecting bolted joint degradation: theory and experiment, Journal of Sound and Vibration 275 (2004) 1113 - 1126.

[11] I. Kajiwara, D. Miyamoto, N. Hosoya, C. Nishidome, Structural health monitoring by high frequency vibration measurement with non-contact laser excitation, Proceedings of SPIE Smart Structures/NDE 2011 (2011) No. 7984-54.

[12] I. Kajiwara, and N. Hosoya, Vibration testing based on impulse response excited by laser ablation, Journal of Sound and Vibration 330 (2011) 5045 - 5057.

[13] N. Hosoya, I. Kajiwara, T. Hosokawa, Vibration testing based on impulse response excited by pulsed-laser ablation: measurement of frequency response function with detection-free input, Journal of Sound and Vibration 331 (2012) 1355 - 1365.

[14] D. Shang, M.E. Barkey, Y. Wang, T.C. Lim, Fatigue damage and dynamic natural frequency response of spot-welded joints, Proceedings of 2003 SAE World Congress, (2003) No. 2003-01-0695.

[15] J. E. Shigley, Mechanical Engineering Design Eight Edition, McGraw-Hill (2006).

[16] S. Kawamura, Y. Nagao, R. Katae, H. Minamoto, Construction of finite element model of a bolt jointed structure with high accuracy, Proceedings of Dynamics and Design Conference 2011 (2011) No. 409.

[17] G. Taguchi, S. Chowdhury, and Y. Wu, The Mahalanobis-Taguchi System, McGraw-Hill, 2001.

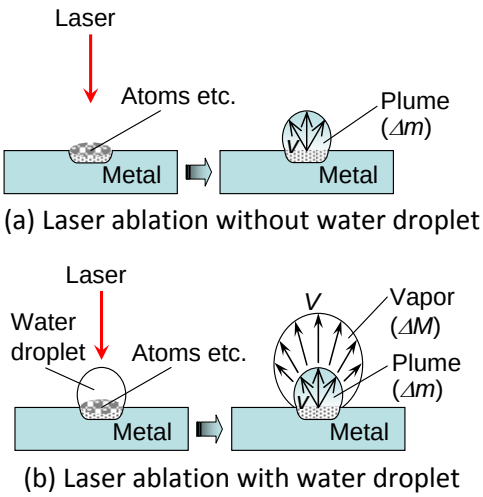

Fig. 1 Process of the laser ablation

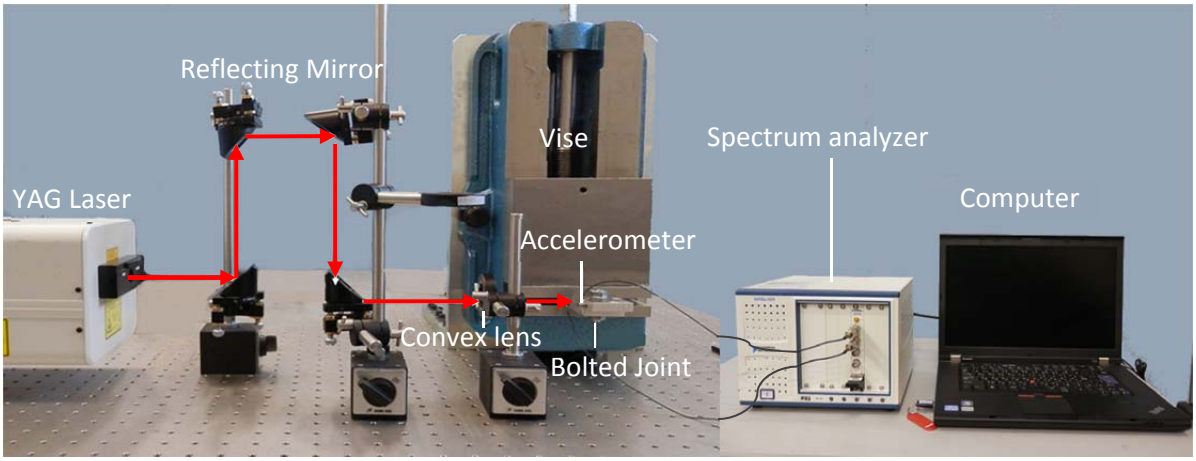

Fig. 2 Vibration testing arrangement using the high power pulse laser

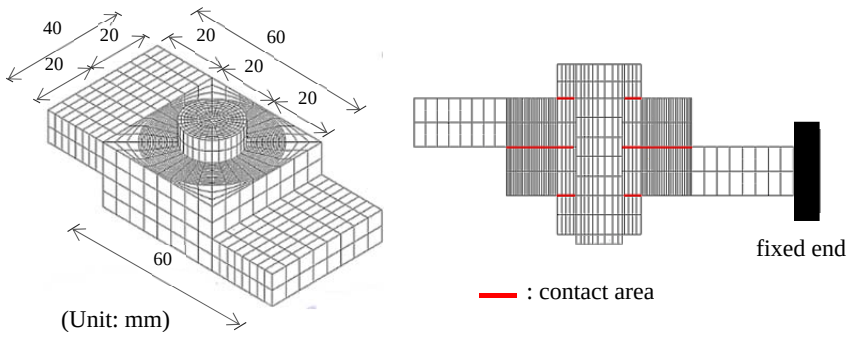

Fig. 3 One-bolt joint model

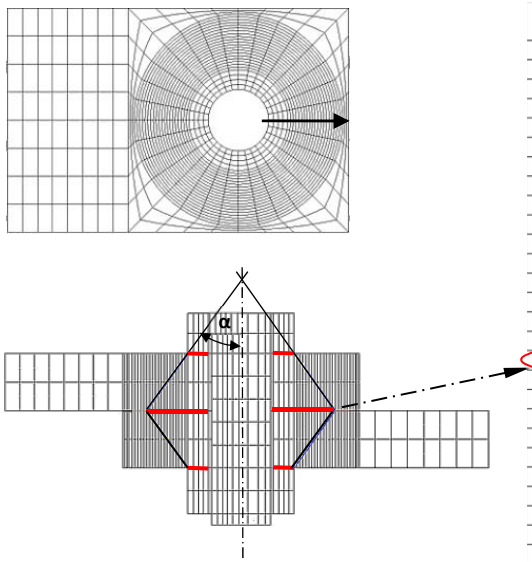

Distance (mm)	Stress on Contact Area For Several Pretension (Pa)				
	12260 N	10000 N	9000 N	7500 N	5000 N
5.5	4.03E+07	3.29E+07	2.96E+07	2.47E+07	1.64E+07
6.25	4.10E+07	3.35E+07	3.02E+07	2.51E+07	1.67E+07
7	3.80E+07	3.09E+07	2.79E+07	2.31E+07	1.55E+07
8	3.65E+07	2.97E+07	2.68E+07	2.23E+07	1.49E+07
9	3.15E+07	2.49E+07	2.31E+07	1.93E+07	1.28E+07
9.5	3.47E+07	2.82E+07	2.50E+07	2.11E+07	1.41E+07
10	2.53E+07	2.03E+07	1.85E+07	1.54E+07	1.01E+07
10.5	2.26E+07	1.88E+07	1.69E+07	1.41E+07	9.49E+06
11	2.11E+07	1.72E+07	1.55E+07	1.29E+07	8.62E+06
11.5	1.95E+07	1.59E+07	1.43E+07	1.19E+07	7.94E+06
12	1.78E+07	1.46E+07	1.32E+07	1.09E+07	7.28E+06
12.5	1.64E+07	1.33E+07	1.20E+07	9.97E+06	6.69E+06
13	1.49E+07	1.22E+07	1.10E+07	9.07E+06	6.01E+06
13.5	1.34E+07	1.10E+07	9.95E+06	8.34E+06	5.52E+06
14	1.23E+07	1.00E+07	9.02E+06	7.52E+06	5.04E+06
14.5	1.13E+07	9.10E+06	8.25E+06	6.83E+06	4.59E+06
15	1.03E+07	8.31E+06	7.54E+06	6.23E+06	4.19E+06
15.5	9.47E+06	7.72E+06	6.95E+06	5.75E+06	3.86E+06
16	8.78E+06	7.12E+06	6.44E+06	5.34E+06	3.56E+06
16.5	8.12E+06	6.60E+06	5.97E+06	5.00E+06	3.32E+06
17	7.62E+06	6.15E+06	5.57E+06	4.64E+06	3.11E+06
17.5	7.20E+06	5.83E+06	5.26E+06	4.38E+06	2.92E+06
18	6.80E+06	5.51E+06	4.99E+06	4.15E+06	2.78E+06
18.5	6.52E+06	5.34E+06	4.81E+06	4.01E+06	2.67E+06
19	6.44E+06	5.25E+06	4.73E+06	3.93E+06	2.62E+06
19.3	6.48E+06	5.32E+06	4.78E+06	3.98E+06	2.67E+06
19.67	6.94E+06	5.68E+06	5.06E+06	4.21E+06	2.81E+06
20	8.05E+06	6.47E+06	5.83E+06	4.93E+06	3.29E+06

Fig. 4 Procedure to determine the benchmark for bonded area

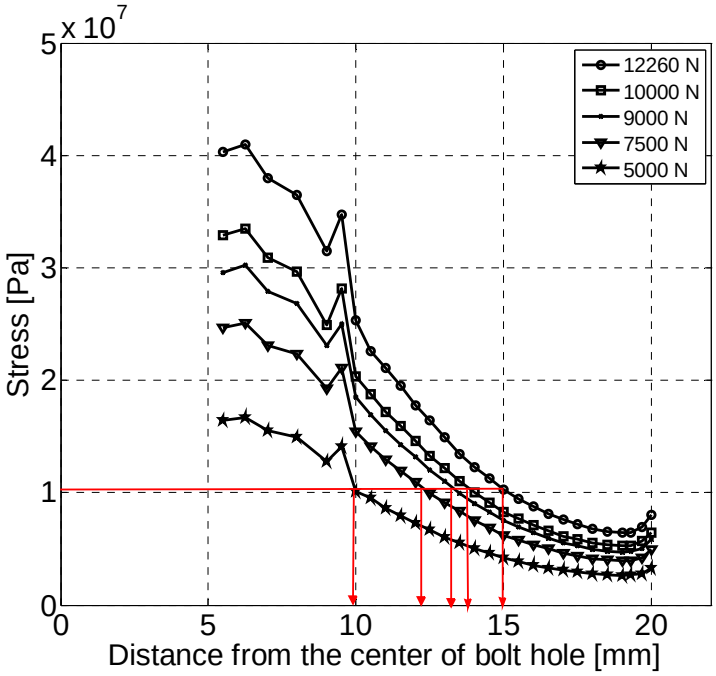

Fig. 5 Stress distribution between flanges in contact for determining bonded contact condition

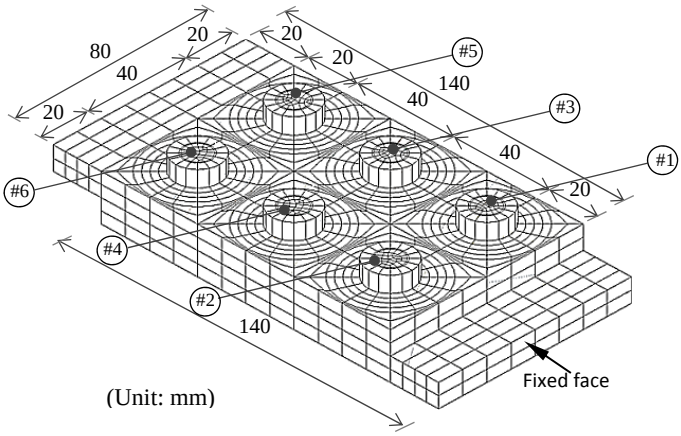

Fig. 6 Six-bolt joint model

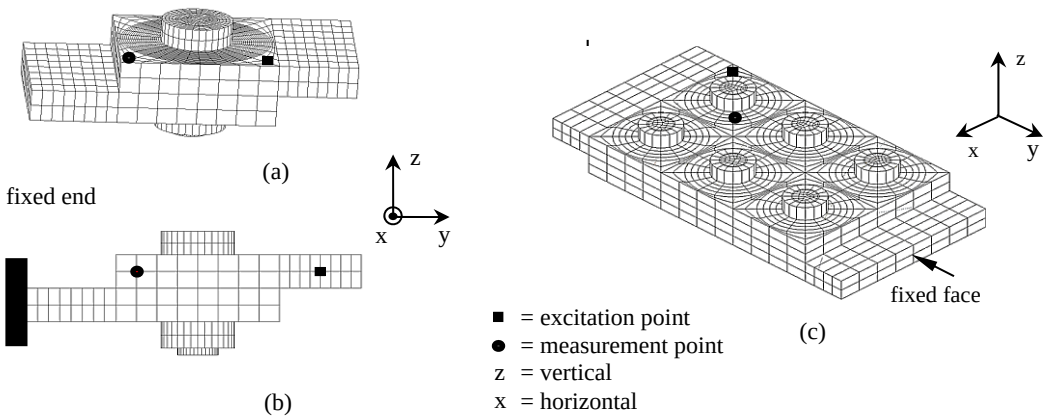

Fig. 7 Excitation and measurement points for verification of the model
(a) vertical of the one-bolt joint, (b) horizontal of the one-bolt joint, (c) vertical of the six-bolt joint

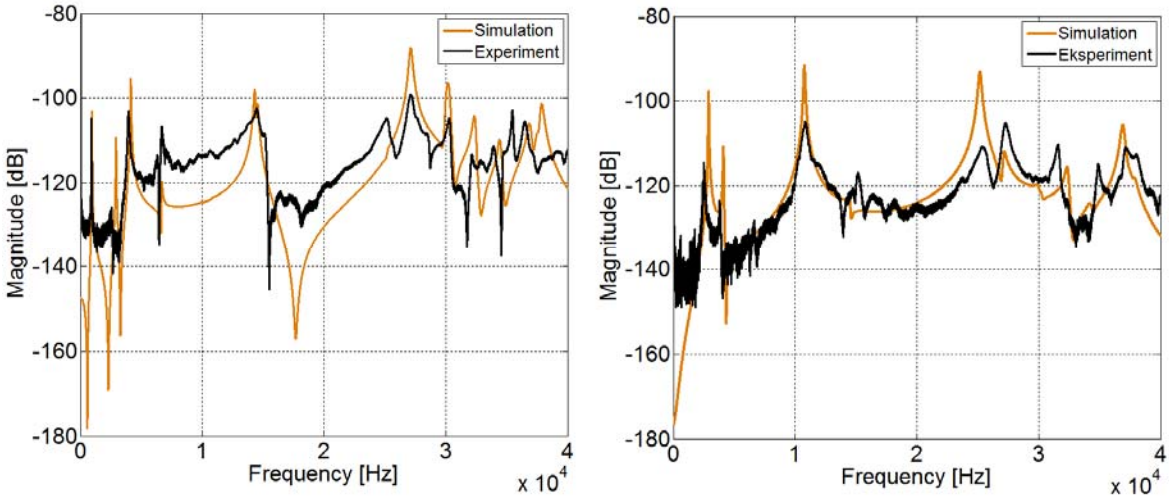

(a) (b)

Fig. 8 Frequency response of the one-bolt joint in the normal condition
(a) in the vertical direction, (b) in the horizontal direction

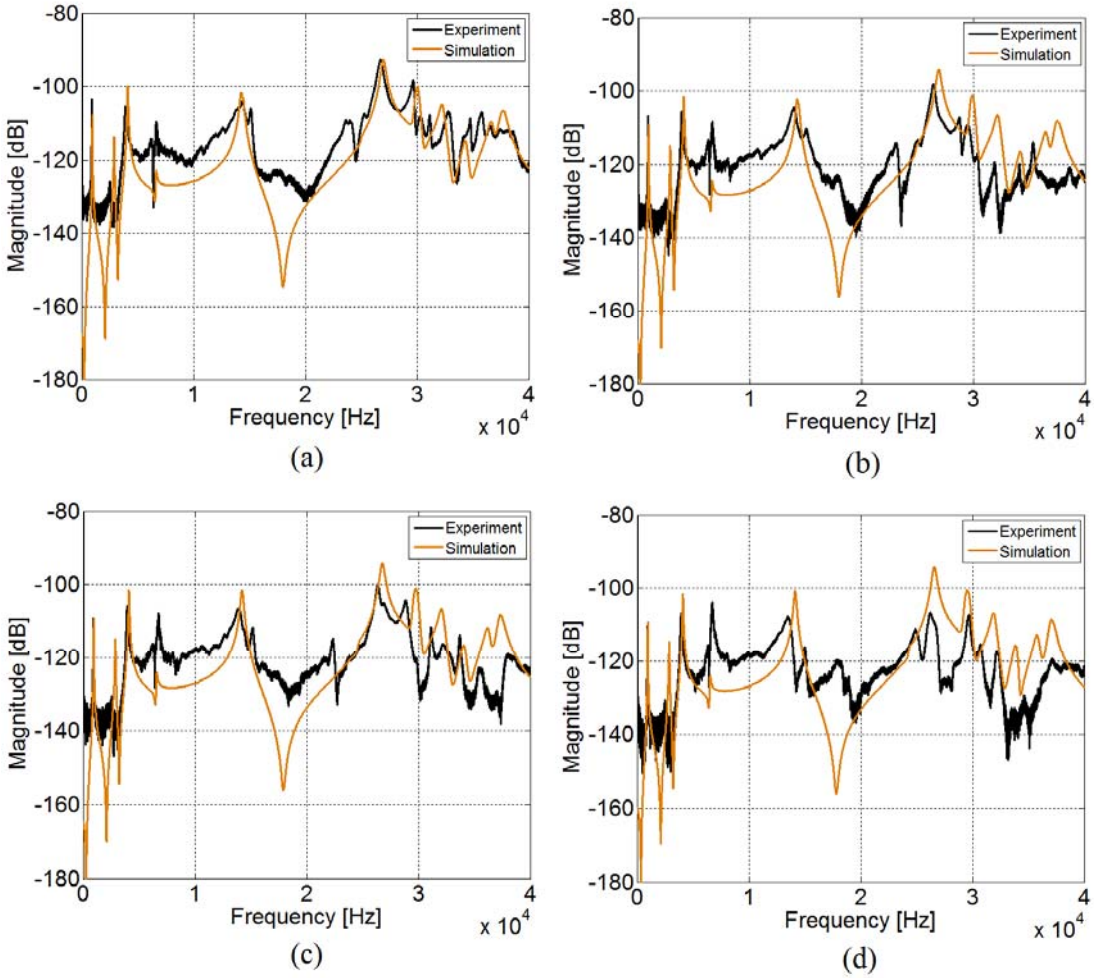

Fig. 9 Frequency response of the one-bolt joint in the vertical direction with the loose condition of tightening torques (a) 20 Nm, (b) 18 Nm, (c) 15 Nm, (d) 10 Nm

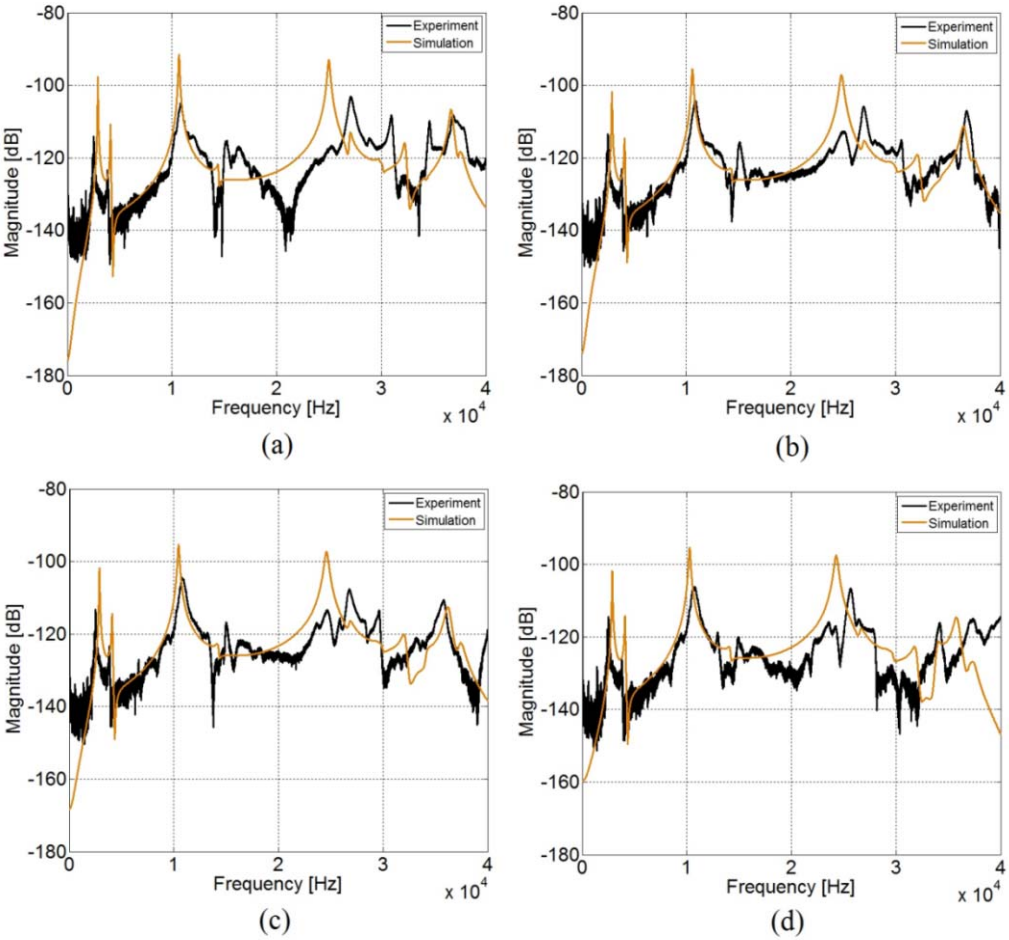

Fig. 10 Frequency response of the one-bolt joint in the horizontal direction with the loose condition of tightening torques (a) 20 Nm, (b) 18 Nm, (c) 15 Nm, (d) 10 Nm

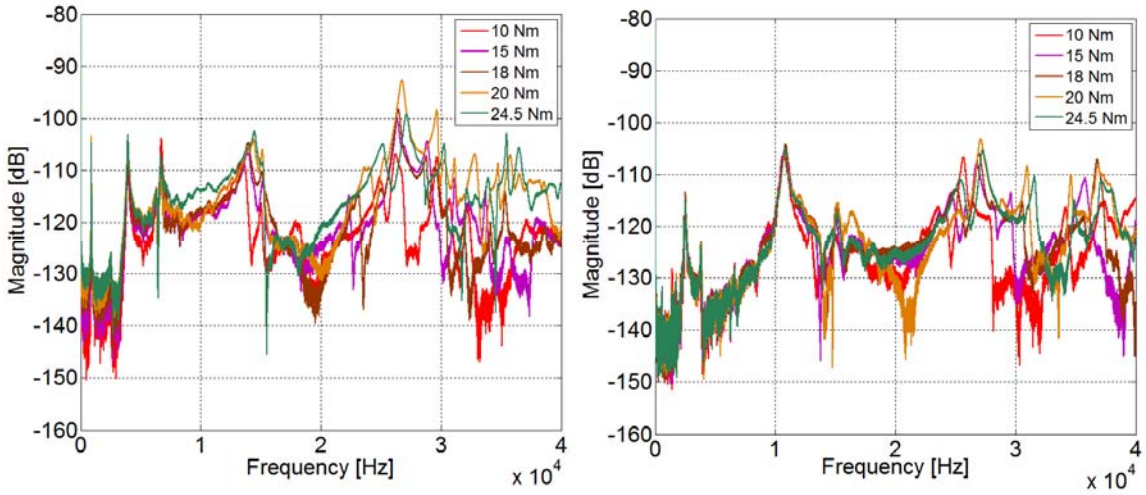

(a) (b)

Fig. 11 Frequency response of the one-bolt joint by the experiments
(a) in the vertical direction, (b) in the horizontal direction

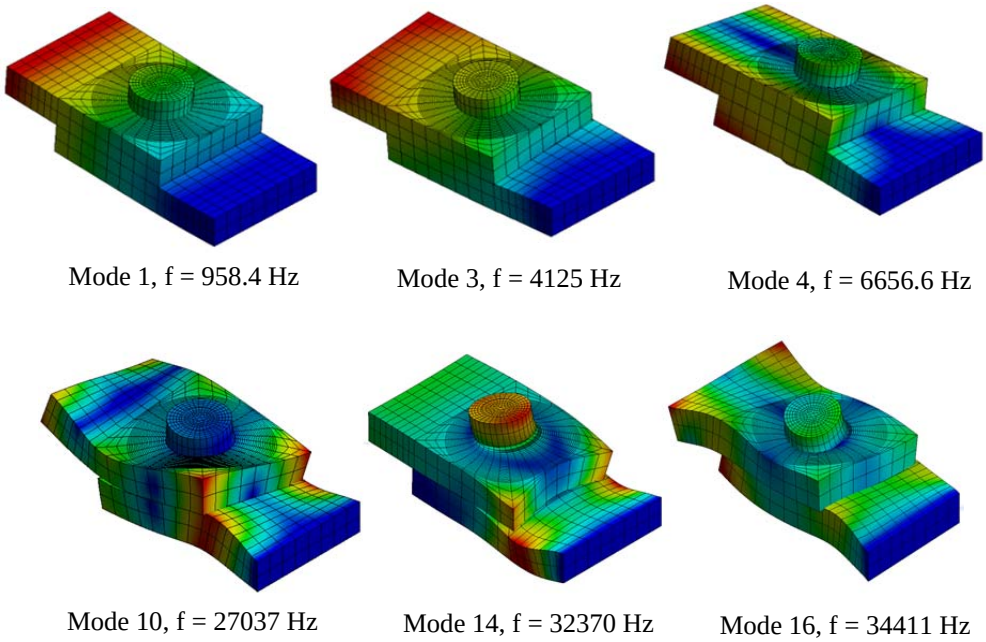

Fig. 12 Principal vibration mode shapes of the one-bolt joint model in the normal condition

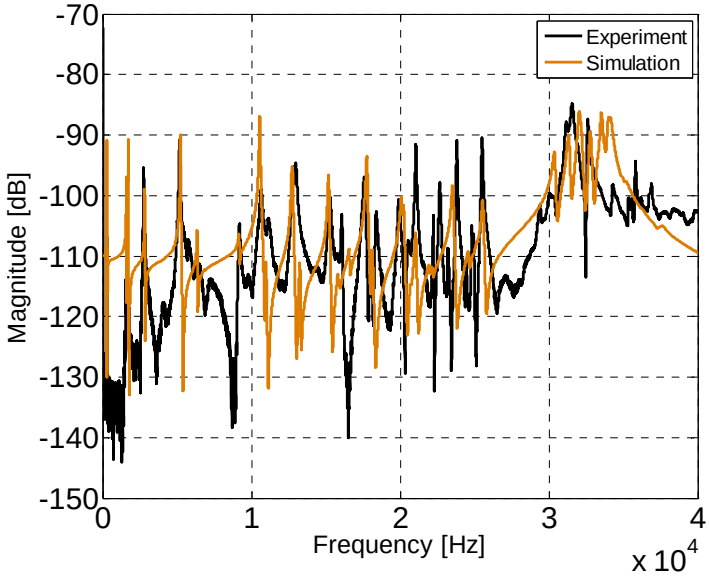

Fig. 13 Frequency response of the six-bolt joint in the normal condition

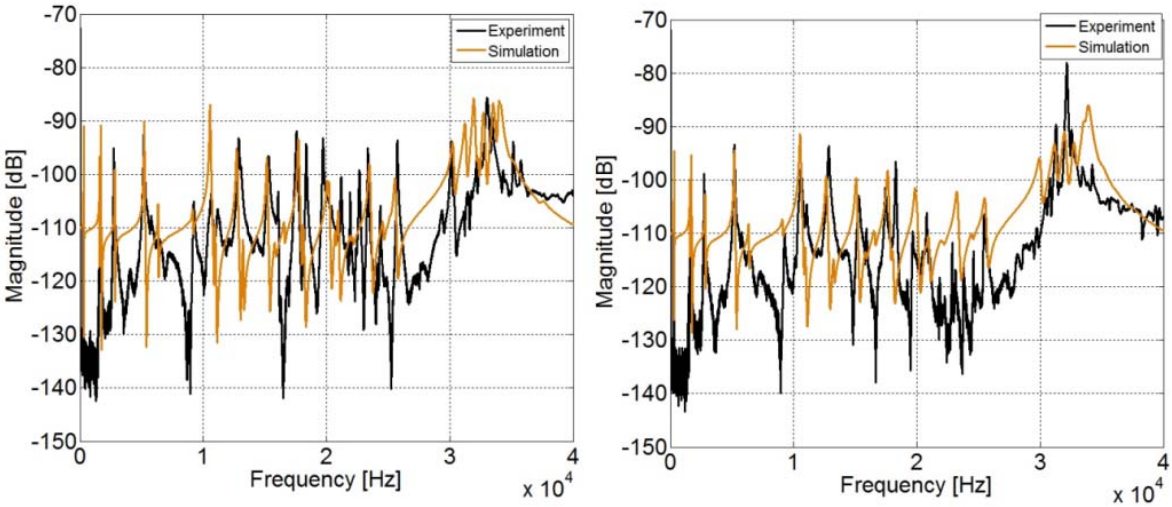

(a) (b)

Fig. 14 Frequency response of the six-bolt joint in loose condition based on damage cases in Table 2 (a) damage 1, (b) damage 5

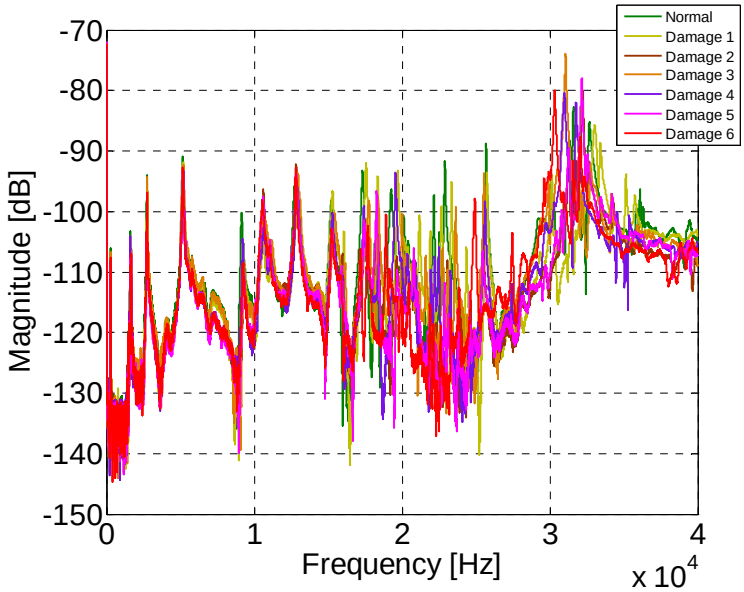

Fig. 15 Frequency responses of the six-bolt joint by the experiments

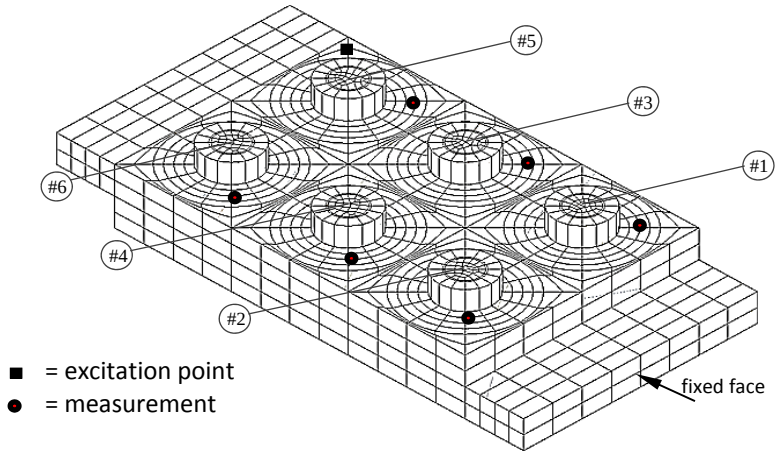

Fig. 16 Excitation and measurement point positions used in bolt loosening detection